Technical Sciences, 2017, 20(4), 343–358

Quarterly peer-reviewed scientific journal
ISSN 1505-4675
e-ISSN 2083-4527
TECHNICAL SCIENCES
Homepage: www.uwm.edu.pl/techsci/

A CFD MODEL OF A TWO-PHASE MIXTURE FLOW IN A TEST STAND FOR AIR-BORNE PARTICLE ANALYSIS

***Marta Stachnik*[1], *Gabriel Czachor*[2], *Marek Jakubowski*[1]**

[1] Department of Food Industry Processes and Facilities
Faculty of Mechanical Engineering
Koszalin University of Technology
[2] Institute of Agricultural Engineering
Wrocław University of Environmental and Life Sciences

Received 12 February 2017, accepted 2 August 2017, available online 16 August 2017.

K e y w o r d s: CFD model, Euler method, two-phase flow, aerosol, air-borne particles.

A b s t r a c t

Farmers come across many materials which when being handled generate dust clouds. Even with low concentration these might pose risk of explosion and can carry dangerous microorganisms. To broaden the knowledge about fine dust particles sedimentation and analyze process of particles becoming air-borne, a tunnel air cleaner was designed. Based on the experiment, a CFX simulation was performed using the Eulerian approach and the CFX12.1 software. Presented model is a stedy state two-phase analysis of dust sedimentation. The results show mechanism of dust dispertion over large distance, such as regions of vorticity that seem to be main motor. Presented analysis emphasizes how easily small particles can become resuspended in the air and carried over distance. Acquired knowledge can be applied for safety regulation in many branches of agriculture.

Nomenclature

C_d – mass density of dispersed phase, kg m^{-3}
d_d – average diameter of particles, μm
D_{md} – diffusion coefficient of dispersed phase in a fluid, m s^{-2}
d_u – unit velocity, m s^{-1}
d_y – unit distance between fluid layers, m
$\mathbf{F}$ – additional volumetric forces, N kg^{-1}
f_d – coefficient of flow resistance for dispersed phase, –
g – gravitational acceleration, m s^{-2}
L – distance in the tunnel, m

Correspondence: Marta Stachnik, Katedra Procesów i Urządzeń Przemysłu Spożywczego, Wydział Mechaniczny, Politechnika Koszalińska, ul. Racławicka 15-17, 75-620 Koszalin, e-mail: marta.stachnik@tu.koszalin.pl

p – pressure, Pa
$\mathbf{u}$ – velocity, m s^{-1}
$\mathbf{u}_{slide}$ – velocity in-between phases, m s^{-1}
μ – dynamic viscosity, Pa·s
μ_T – turbulent viscosity, Pa·s
ν – kinematic viscosity, m^2 s^{-1}
ρ – density, kg m^{-3}
ρ_c – density of solid phase, kg m^{-3}
ρ_d – density of dispersed phase, kg m^{-3}
τ – shear stress, N m^{-2}
φ_c – volumetric share of continuous phase, –
φ_d – volumetric share of dispersed phase, –

Introduction

Handling solid material produces clouds of dust. Dust particles are not only a threat to health, but also pose a fire and explosion hazard. An airborne powder of a combustible material has properties similar to a flammable gas mixed with air, and so it can cause an explosion in a closed space. Furthermore, pressure waves from the initial explosion can throw deposited dust into the air in front of the advancing flame, all of which may result in a "secondary" explosion, extending far beyond the original dust cloud (*Hazard Prevention and Control*... 1999). Air cleaning equipment has to be installed everywhere where dust clouds are generated. Selection of a dust control system is based on the desired air quality. The dust control system is required to prevent or minimize the risk of an explosion or fire, and to reduce employee exposure to dust. Moreover, these installations deal with unpleasant odors, improve visibility and lower the probability of an accident (FLAGAAND, SEINFELD 1988, *Hazard Prevention and Control*... 1999).

Farmers deal with many types of biomass that generates dust – fertilizers, forage, wheat, straw or wood chips. Pellets have become very popular for household use, all sorts of straw, wood chips or biomass mix can be used as raw materials. Still, the most common one is straw, because it is usually collected instead of being mixed with the soil. Then it can be used for burning in boilers, either in the form of bales or pellets (OBERNBERGER, THEK 2010, DÖRING 2013).

Computer simulations have become a very useful tool. More and more processes are analyzed using CFD (Computational Fluid Dynamics) simulations. CFD is a proven simulation tool, and it is applicable to almost any field of study. It can be applied to various agricultural issues, such as external atmospheric processes as well as modeling in land and water management, predicting forest fires, air pollution and dust dispersion (LEE et al. 2013).

Although there have been numerous attempts at modeling the sedimentation process, there are still some unresolved issues. DORRELL and HOGG (2010)

mathematically modeled sedimentation of bidisperse suspensions in quiescent fluid. Sedimentation process of non-cohesive solid particles in a two-dimensional channel was also modeled by XU and MICHAELIDES (2003). They analyzed particle behavior in a horizontal channel. The simulations showed that the process of sedimentation comprises three stages. During the first stage, the initial particle configuration has key influence on the average velocity of particles and they might form a *V*-shape or *W*-shape front. In the second stage concentration of particles is lower, but strong interactions occur among them. The process highly depends on the formation and destruction of particle clusters. The sedimentation velocity depends on the number of clusters formed and developed velocity field. During the third stage, the concentration becomes low and the particle clusters become stable (XU, MICHAELIDES 2003).

This paper is focused on creating a CFD model of a horizontal tunnel (Fig. 1) using CFX software package. This tunnel will be used to analyze sedimentation of dust to improve modern air cleaning systems. Moreover, the tunnel will be used to analyze the process in which fine particles become airborne, since the majority of research in the field of agriculture focuses on larger ones, such as grains and seeds and not on the fine particles or dust.

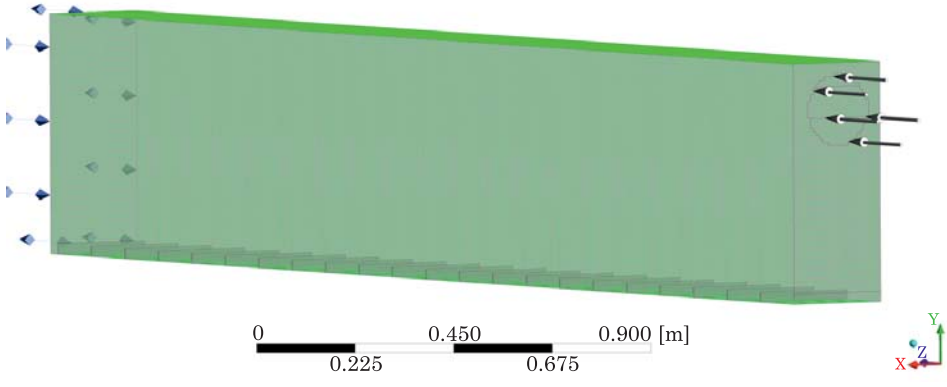

Fig. 1. The geometry of the simulated tunnel and applied mesh

Material and methods

The object of the simulation is a box-shaped tunnel (Fig. 2). Specifications needed for creating three-dimensional model, the computational simulation and validation of the results were obtained in association with The Wrocław University of Environmental and Life Sciences.

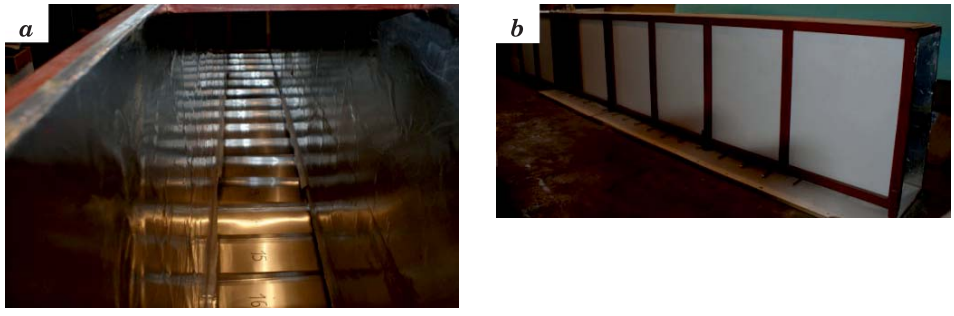

Fig. 2. The experimental tunnel: *a* – view of the sections at the bottom, *b* – general view

Experiment setup

The experiment was performed in a full scale tunnel of the same dimensions as the one used for simulation (Fig. 2). In Figure 3 sections at the bottom are shown. The air was polluted with dust generated during straw pellet production. Analysis of the dust particles' geometry showed that only 10% had their shape close to spherical – for instance index of sphericity higher than 0.9 (CZACHOR et al. 2014). Mastersizer 2000 (Malvern Instruments, UK) was used for measuring particle size of the dust. These measurements were later used to set properties of the simulated dust. Its working principle is based on laser

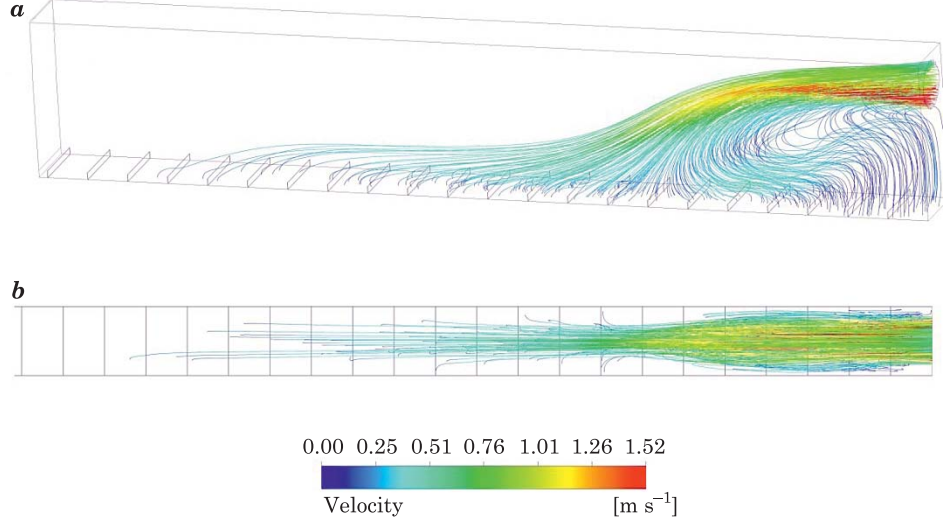

Fig. 3. Particle velocity on particle trace visualization for 300 pcs: *a* – side view, *b* – top view

diffraction. When particles pass through a focused laser beam they scatter light at an angle that is inversely proportional to their size. This angular intensity of the scattered light is measured by a series of photosensitive detectors, providing the final result.

Mathematical model

Based on an Eulerain description of the phases, a two-phase model is presented. The considered flow is steady. The equation of continuity for the flow is formulated by applying the principle of mass conservation to a small volume of fluid. The standard form of this equation for Cartesian coordinates goes as follows (ABBOTT, BASCO 1989):

$$\nabla \cdot (\rho \mathbf{u}) = 0 \tag{1}$$

The velocity distribution of a dispersed phase is represented by the following equation (ABBOTT, BASC 1989, pp. 5–30):

$$\nabla \cdot \varphi_d \left[\mathbf{u} + \varphi_d (1 - c_d) \mathbf{u}_{\text{slide}} - \frac{D_{md}}{\varphi_d} \nabla \varphi_d \right] = - \frac{m_{dc}}{\rho_d} \tag{2}$$

Equation of momentum takes the form of (ABBOTT, BASCO 1989, JAKUBOWSKI et al. 2014):

$$\begin{aligned} \rho \mathbf{u} \cdot \nabla \mathbf{u} = & - \nabla [- p + (\mu + \mu_T)(\nabla \mathbf{u} + (\nabla \mathbf{u})^T)] - \\ & - \nabla \cdot \{ [\rho c_d (1 - c_d) [\mathbf{u}_{\text{slide}} \mathbf{u}_{\text{slide}}\} + \rho \boldsymbol{g} + \mathbf{F} \end{aligned} \tag{3}$$

where

$$\rho = \varphi_c + \varphi_d \rho_d \tag{4}$$

and

$$c_d = \frac{\varphi_d \rho_d}{\rho} \tag{5}$$

A fluid-fluid drag function is modeled using the Schiller-Neumann model, which is specified with the following equation:

$$\frac{3 f_d}{4 d_d \cdot 10^{-6}} \rho_c \, |\mathbf{u}_{\text{slide}}| \, \mathbf{u}_{\text{slide}} = \frac{\rho - \rho_d}{\rho} \nabla_p \tag{6}$$

Schiller-Neumann model is the one available for modeling fluid-particle interaction. This is valid model widely used and giving suitable results. It is used for particles that are sufficiently small and considered spherical. Moreover, this model is suitable for sparsely distributed particles.

The correct limiting behavior in the inertial regimes is ensured by limitation of Reynolds number as follows:

$$f_d = \begin{cases} \dfrac{24}{\mathrm{Re}_p}\left(1 + 0.15\ \mathrm{Re}_p^{0.687}\right) & \text{for } \mathrm{Re}_p < 1000 \\ & \text{for } Re_p > 1000 \end{cases} \tag{7}$$

where Reynolds number is defined as:

$$\mathrm{Re}_p = \frac{d_d \cdot 10^{-6} \rho_c \left|\mathbf{u}_{\mathrm{slide}}\right|}{\mu} \tag{8}$$

For turbulence a standard κ–ε model was used (ZIKANOV 2010, JAKUBOWSKI et al. 2014). It was chosen as it is useful and accurate for free-shear layer flow with relatively small pressure gradient and wall-bounded and internal flow. This model includes two extra transport equations to represent the turbulent properties of the flow. This allows a two equation model to account for history effects like convection and diffusion of turbulent energy. The turbulence kinetic energy (k) is specified with the following equation:

$$\rho \frac{\partial k}{\partial t} + \rho \mathbf{u} \cdot \nabla k = \nabla \cdot \left[\mu + \sigma_k \mu_T \nabla\right] + P_k - \rho \beta \mathrm{k} \omega \tag{9}$$

For dissipation the model transport equation can be written as:

$$\rho \frac{\partial \varepsilon}{\partial t} + \rho \mathbf{u} \cdot \nabla \varepsilon = \nabla \cdot \left[\left(\mu + \frac{\mu_T}{\sigma_\varepsilon}\right) \nabla \varepsilon\right] + C_{\varepsilon 1} \frac{\varepsilon}{k} P_k - \rho C_{\varepsilon 2} \frac{\varepsilon^2}{k} \tag{10}$$

Where P_k represents the rate of shear production of k and is given in expanded form as follows:

$$P_k = \mu_T \left(\left[\frac{\partial \mathbf{u}}{\partial y} + \frac{\partial v}{\partial x} \right]^2 + \left(\frac{\partial v}{\partial z} + \frac{\partial \mathbf{w}}{\partial y} \right)^2 + \left(\frac{\partial \mathbf{u}}{\partial z} + \frac{\partial \mathbf{w}}{\partial x} \right)^2 \right] + \mu_T \left[2 \left(\frac{\partial \mathbf{u}}{\partial x} \right)^2 + 2 \left(\frac{\partial v}{\partial y} \right)^2 + 2 \left(\frac{\partial \mathbf{w}}{\partial z} \right)^2 \right. \tag{11}$$

and eddy viscosity is modeled as:

$$\mu_T = C_\mu \frac{k^2}{\varepsilon} \tag{12}$$

Computational model assumptions

Studied flow was steady and subsonic. The flow was assumed to be incompressible as there was no pressure change and temperature changes were neglected. Moreover its physicochemical properties were constant. The process was isothermal and there was no occurrence of chemical reactions and such conditions were applied for experimental study. There was no transfer of mass and momentum at the interface of air and dust. Pressure changes were intentionally omitted as those would not have any influence on the process. Based on observation the turbulence was considered as low (1%). Particles were fully coupled to the continuous fluid. Fully coupled particles exchange momentum with the continuous phase, enabling the continuous flow to affect the particles, and the particles to affect the continuous flow. Full coupling is needed to predict the effect of the particles on the continuous phase flow. The drag force was taken into account, it was based on Schiller-Neumann model. As dust particle is simulated to be of a simple shape and it is immersed in a Newtonian fluid – air, which is not rotating relative to the surrounding free stream, the drag coefficient depends only on the particle Reynolds number. The studied process was sedimentation and so the gravitational effect and buoyancy were considered.

In multiphase flow the difference in density between phases produces a buoyancy force. Analyzed flow contained a continuous phase and a dilute dispersed phase, so the value of the buoyancy reference density was set of the continuous phase. This is because the pressure gradient is nearly hydrostatic, so the reference density of the continuous phase cancels out buoyancy and pressure gradients in the momentum equation.

The domain's boundary conditions were set to: reference pressure – 1 atm; gravity – 9.81 m s^{-2} and buoyant reference density was set as 1 kg m^{-3}. The wall boundary conditions were set to no-slip wall option and smooth wall. The fluid layer at the wall had velocity equal to that on the wall. For steady state this velocity was zero:

$$\mathbf{u} = 0 \tag{13}$$

CFD distinguishes between two Coefficients of Restitution specifying particle behavior after collision: parallel coefficient of restitution – was set as 0; and perpendicular coefficient of restitution was set as 0.5, thus particles collision was semi-elastic. The parallel and perpendicular restitution coefficients describe the action of particles when they hit a wall. Dust particles did not stick to the wall nor did they bounce off immediately.

As for initial conditions for air, temperature at the inlet was set to 25°C. In the experiment air velocity was non-uniform. Boundary "Inlet" in the CFD model was divided in three sections, where measured values were applied. For top section: velocity was set at 0.60 m s^{-1}, mass flow rate of $2 \cdot 10^{-5}$ kg s^{-1}. Middle section: velocity was 0.9 m s^{-1}, mass flow rate of $3 \cdot 10^{-5}$ kg s^{-1}. Bottom section: velocity was 1.5 m s^{-1}, mass flow rate of 10^{-4} kg s^{-1}. Particle diameter distribution was based on normal distribution and the flow was uniform.

Relative pressure for opening was set to 0 Pa, what means that at the exit pressure was 1 atm.

Convergence was achieved when the RMS (Root Mean Square) of the normalized residual error reached the value of 10^{-4} for all the equations. This required 1820 loop iterations.

CFD Model

The overall dimensions of the device were: width 0.3 m, depth 4 m, and height 0.7 m (Fig. 1). The center of a round inlet was situated at the height of 0.6 m, and its diameter was 0.14 m. The cleaner was graduated in each dimension with marks for each: 0.3 m along the width (across the bottom of the box), 0.03 m along the height, and 0.18 m along the length.

Properties of the simulated dust were set to: min. diameter 28 μm, max. diameter 64 μm, mean diameter 44 μm, S_d 13 μm and density of 700 kg m^{-3}. Mean distribution of particles' diameters was based on Gaussian distribution. The geometry of the flow domain was created in Cartesian coordinates (X, Y, Z). The length of the tunnel followed the Z axis, width – the X axis, and height – the Y axis. Mesh was created with the meshing tool available as part of ANSYS, and it had 931,023 nodes and 88,420 elements. A structured grid was chosen, so that cells would be hexahedral and would not skew. The domain was divided into the hexahedral mesh. The domain consisted of three boundaries: inlet, outlet and wall. The inlet was divided into three regions. This classification was the result of non-uniform distribution of particles and their velocity at the entrance.

Results and discussion

In turbulent flow there are two well understood mechanisms that influence the mean settling rate. The firsts is due to the non-linear dependence of the drag on the relative velocity at finite Reynolds numbers. The settling velocity decreases with increasing turbulence intensity. The second mechanism is more complex and is due to the preferential trajectories of freely falling particles. Particles do not sample the turbulent flow infirmly, but prefer regions of downwash rather than regions of the up-moving fluid. Particle movement is also influenced by the velocity of the fluid, friction between particle and air and force of gravity.

Particles entered the inlet with the air stream and followed its trajectory. The particle velocity profile is shown in Figure 3 and the velocity profile of the mixture is presented in Figure 4. Dust entered the cleaner at 1.5 m s^{-1} at the bottom of the inlet, 0.9 m s^{-1} in the middle and 0.6 m s^{-1}at the top section of the inlet. Due to gravitational force and air friction, particles lost their velocity and settled at the bottom of the box. Streamline indicated two regions of turbulence (Fig. 5). The swirl that appeared over the stream had no influence on the particles' trajectory. Velocity in this region had average value of 0.27 m s^{-1}. Under the stream at the distance of 1 m a turbulent flow occurred, that carried particles backward. The average velocity of that air whirl was 0.46 m s^{-1}, ranging from 0.53 to 0.36 m s^{-1}. The carried particles lost their velocity to average 0.04 m s^{-1} and settled within the first five sections. Illustration in Figure 3*b* shows that particles formed a *U*-shaped front. This was caused by the horizontal motion of the stream, as opposed to vertical motion which causes formation of a *V*- or *W*-shape front. Three stages mentioned in the introduction and studied by XU and MICHAELIDES (2003) can be partially observed in analyzed flow. Particles initially create uniform flow and it is consistent with initial configuration, meaning that air velocity has strongest affect on particle behavior and here the *U*-shaped front can be observed. The shape resembling more letter *U* than *V* is caused by the horizontality of the flow. Vertical flow creates sharper edges as gravity adds to the flows shape, in analyzed flow gravity worked against it. At the second stage gravity has stronger influence than air, particle clusters become less dense, but no strong interactions occur among them. During the third stage the concentration becomes the lowest. The sedimentation velocity depends rather on strength of the influence of the gravity rather than on the number of clusters formed. Even though there is discrepancy between horizontal and vertical flows particles behave similarly. Heavier particles went off the stream's course immediately, and lighter ones created a rounded front. Dust that entered through the top section of the inlet had an average velocity of 0.6 m s^{-1}, but it

was carried by the lower faster stream and those particles accelerated up to between 0.83 and 0.91 m s^{-1} (average) and then slowly descended. Due to friction between the air stream and the edges of inlet, velocity was much lower – average 0.62 m s^{-1}.

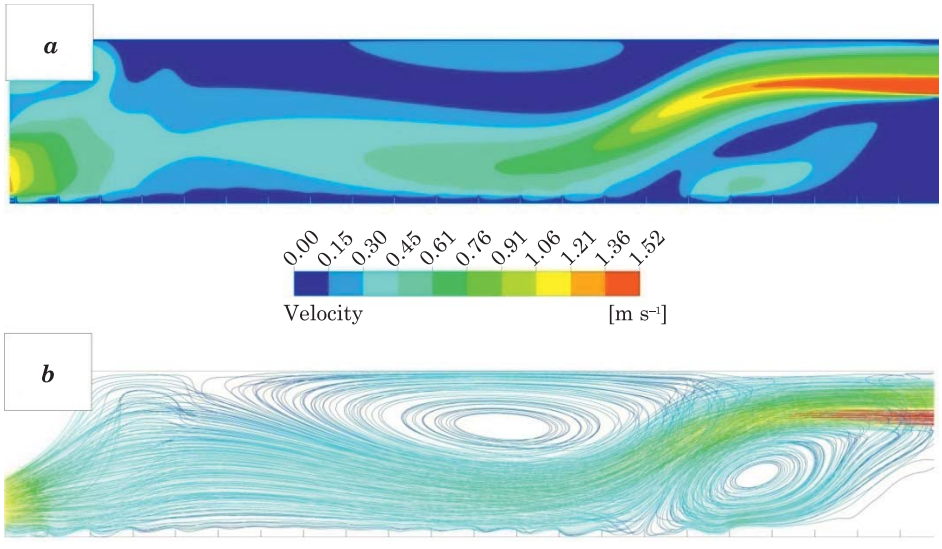

Fig. 4. Velocity in the tunnel: *a* – velocity profile in *ZY* plane for $X = 0.15$ m, *b* – velocity vector plot on a streamline

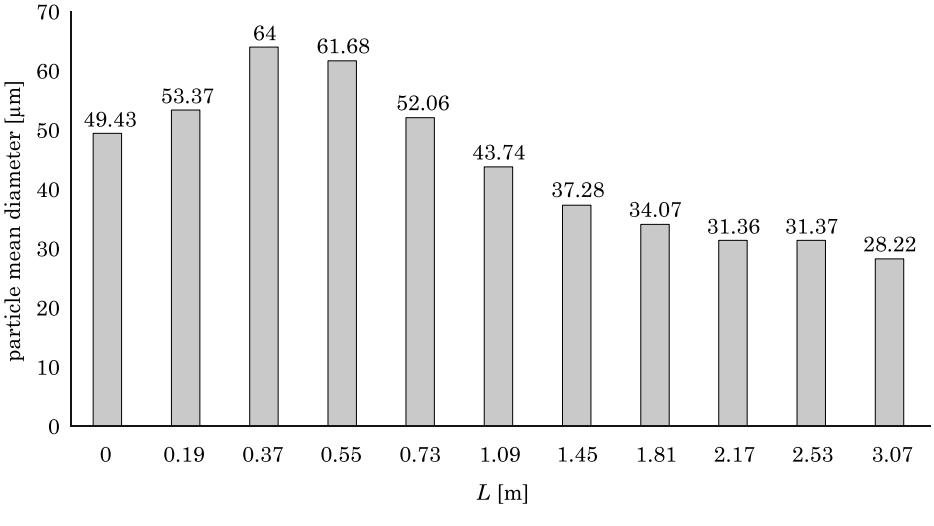

Fig. 5. Experimental mean particle diameter distribution along the tunnel, *L* – length of the tunnel

The first attempt at model verification was done by comparing the velocity distribution. Three planes were placed at specific distances from the inlet – the same ones at which measurements in the tunnel were conducted. Experimental results are listed in the Table 1 and results from computational model are concluded in the Table 2.

Table 1

Velocities measured in the experimental tunnel

Distance from inlet [m] / Height above bottom [m]	Velocity [m s^{-1}]		
	0.10	2.10	3.00
0.10	0.44	0.36	0.31
0.30	0.39	0.53	0.36
0.45	0.45	0.61	0,36
0.60	0.90	0.45	0.25

Table 2

Velocities from CFD model of the tunnel

Distance from inlet [m] / Height above bottom [m]	Velocity [m s^{-1}]		
	0.10	2.10	3.00
0.10	0.02	0.52	0.20
0.30	0.06	0.38	0.33
0.45	0.40	0.07	0.20
0.60	0.90	0.19	0.04

Close to the inlet there was a discrepancy between the calculated and measured velocity. It was due to dividing the inlet into three sections, each having a different velocity, and so air stream in the simulation achieved its uniform velocity later than in the experimental tunnel. Further away from the inlet velocity of the fluid stream was more similar to data presented in the Table 2. Such a discrepancy is a result of simplifications required to perform a computer simulation.

A chi-squared test was conducted, and it showed that there was no significant difference between velocities at 0.10 m and 2.10 m. The critical value for $\alpha = 0.05$ was $p = 0.3519$ and calculated values were $p_{0.10} = 0.01383$ and $p_{2.10} = 0.2009$ respectively. The calculated value of $p_{3.00}$ was equal to 0.7306. Apparently, there was a significant difference between the registered velocities but only at a considerable distance from the inlet.

As predicted, the smallest particles traveled the longest distance, and those of the biggest mean diameter settled at the beginning of the tunnel (Fig. 5, 6). As mentioned before, some particles accumulated within the first few sections because of air stream turbulence.

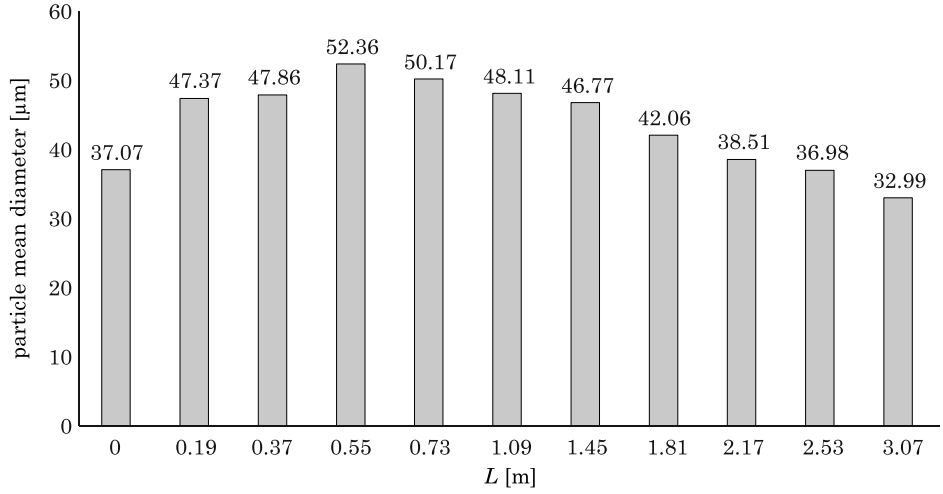

Fig. 6. Simulated particle diameter distribution throughout the tunnel, L – length of the tunnel

Statistic analysis with the use of the chi-square test showed that there was no significant difference between the two distributions. The calculated value p equaled $1.384 \cdot 10^{-6}$ and it was smaller than the critical value $p = 5.226$ for $\alpha = 0.05$. This means that both distributions are similar and CFD model if sufficiently accurate.

Both charts show that the smaller the particle was, the farther it traveled, and the lightest ones went as far as 3.6 meters. Medium-sized particles landed mainly within central segments of the tunnel, but some were carried backward, that is toward the front wall. Particles' mass correlates with their size, thus, mass and mean diameter distributions look similar. The smallest particles were the lightest ones, and they were carried the longest distances by the air stream. Lightest bits of dust had the mean diameter equal to 28.31 μm, and the heaviest particles had the mean diameter of 63.75 μm.

The heaviest particles entered through the bottom and the central parts of the inlet, where the velocity was highest, but they landed soon after. The lightest particles on the other hand came mostly from the top part of the inlet. Despite the fact that their velocity was the lowest they traveled the longest distance due to their small weight – meaning the gravitational pull was weakest, all of which suggests that those particles are the most likely to become airborne. Even the smallest bits can carry pathogenic microbes. WHO classified dust particles into 3 categories: inhalable, thoracic, and respirable fractions. The most dangerous are the respirable ones, because human body is not able to remove them from the air passages (*Hazard Prevention and Control*... 1999). Inhalable fraction consists of particles of the size smaller than 100 μm.

Upper respiratory system: nose, mouth, throat and larynx can stop and remove from the body particles bigger than 30 μm. Particles up to 20 μm reach the middle respiratory system: trachea, bronchi and bronchioles. Respirable fraction consist of particles smaller than 7 μm, those reach alveoli and can stay there up to 3 months (*Hazard Prevention and Control*... 1999). Relative mass distribution was calculated for both experimental and model tunnel and it is presented in Figures 8 and 9 and on the particle track in Figure 7. It can be seen that dust's bits in the CFD model were more evenly distributed along the bottom. Differences between experimental results and data obtained from the CFD analysis come from simplifications implemented in the computational model. Material properties were averaged and humidity of the air and moisture content of the dust were intentionally omitted.

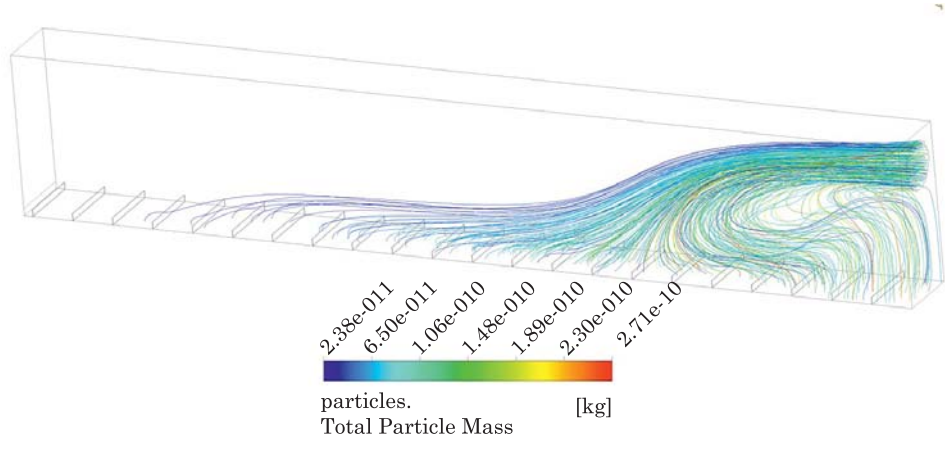

Fig. 7. Particle mass distribution throughout the tunnel

Statistic analysis with the use of the chi-square test showed that there was no significant difference between the experimental and simulated distributions. The calculated value p equaled 0.537 and was smaller than the critical value of 9.380 for $\alpha = 0.05$. Meaning, both series belonged to the same population.

KOCH and HILL (2001) pointed out that particle inertia plays a very important role in the sedimentation process, in fact, it leads the particles to be thrown out of vortices and to accumulate in regions where the turbulence is lower. This is one of the mechanisms on how particle clusters are formed and sustained. It held true for the analyzed case. As shown in Figure 4*b* there was a vortex under the stream, which pulled back some of the particles to the front of the tunnel (Fig. 8). Moreover, inertia pushed the lightest particles forward.

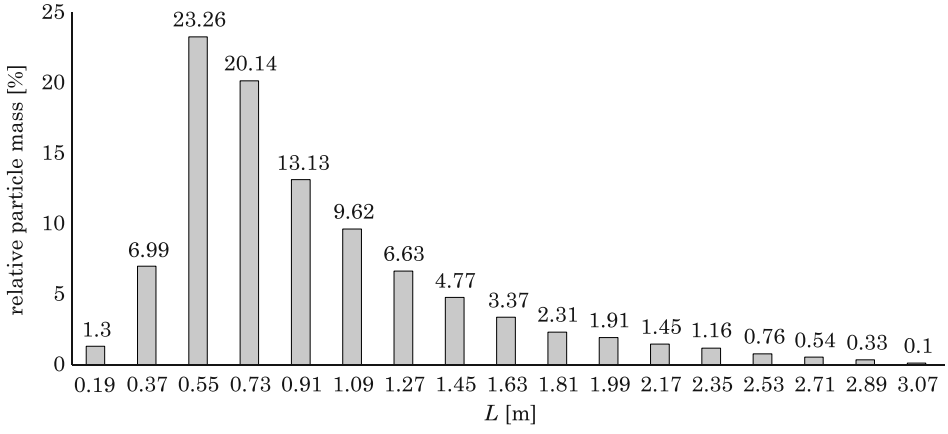

Fig. 8. Experimental relative particle mass distribution throughout the tunnel, L – length of the tunnel

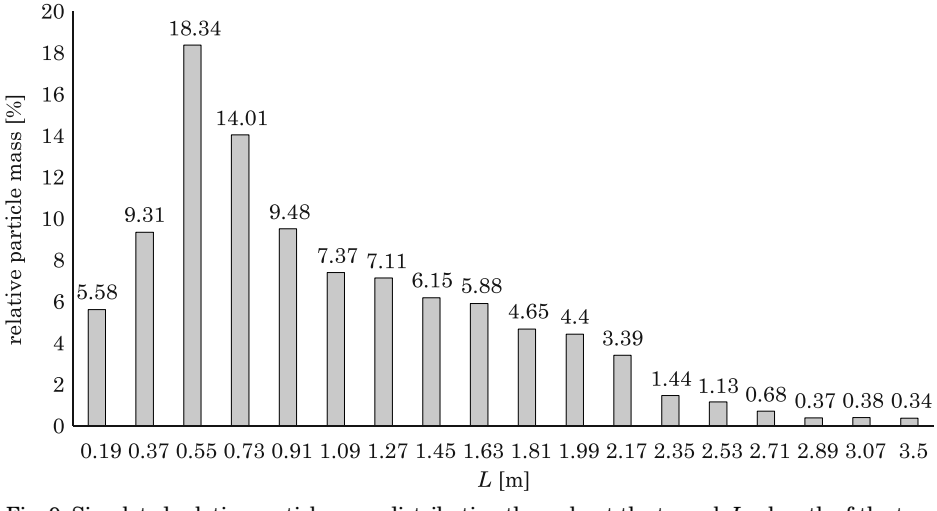

Fig. 9. Simulated relative particle mass distribution throughout the tunnel, L – length of the tunnel

The top of the air stream had lower velocity, however, because of the lower layer having higher velocity, the smallest bits traveled all the way to the exit of the tunnel.

Air streams can occur anytime during when farm materials are being handled, e.g. door opening or in a straw cutter. Moving air even at the speed of 0.6 m s^{-1} can put dust particles in motion. Dust deposits might be moved at a significant distances (here 3 m). In the tunnel air vortexes appeared, those can give insight in particle behavior in highly turbulent air stream.

Conclusions

In this paper a 3D numerical model was used to simulate the flow structure of a horizontal tunnel taking into account the momentum exchange between particles and fluid phase. The verified computational model is accurate. Results obtained via calculations show significant similarity to those from the experiment in terms of particle distribution along the bottom of the tunnel. This proves that simulation was carried out in an appropriate manner and can be used for further investigation. Three important characteristics, gravitational settling and deposition and resuspentions, of particles are included and considered carefully. The simulation results show that gravity has a noticeable influence on larger particles, but for smaller particles the influence of gravity is small and, in general, they share the common dispersion and transport properties of air. The model is extensible to consider more physical effects, such as thermal gradient, pressure changes, surface roughness, electrostatic forces and particle resuspension. As there is lack of simiral analysis presented model will be used to simulate motion and behavior of particles of different size and density found in field of agriculture.

References

Abbott M.B., Basco D.R. 1997. *Computational Fluid Dynamics: An Introduction For Engineers*. Longman Group, UK Limited, p. 5–30.

Cecala A.B., O'brien A.D., Schall J., Colinet J.F., Fox W.R., Franta R.J., Joy J., Reed W.R., Reeser P.W., Rounds J.R., Schultz M.J. 2012. *Report of Investigations 9689 Dust Control Handbook for Industrial Minerals Mining and Processing, Centers for Disease Control and Prevention National Institute for Occupational Safety and Health Office of Mine Safety and Health Research Pittsburgh*. http://www.cdc.gov/niosh/mining/UserFiles/works/pdfs/2012-112.pdf, p. 28–42 (access: 20.10.2014).

Czachor G., Bohdziewicz J., Gryszkin A. 2014. *Analysis of the size of dust particles which were formed during pellet production*. Inżynieria Rolnicza, 2(150): 7–13.

Döring S. 2013. *Power from Pellets Technology and Applications*. Springer, p. 13–14.

Dorrell R., Hogg A.J. 2010. *Sedimentation of bidisperse suspensions*. International Journal of Multiphase Flow, 36: 481–490.

Flagan R.C., Seinfeld J.H. 1988. *Fundamentals of Air Pollution Engineering*. Prentice-Hall Inc., US, http://authors.library.caltech.edu/25069/ p. 391–478 (access: 21.10.2014).

Hazard Prevention and Control in the Work Environment: Airborne Dust. Protection of the Human Environment Occupational Health and Environmental Health Series. 1999. Geneva Hazard prevention and control in the work environment: Airborne dust. http://www.who.int/occupational_health/publications/en/oehairbornedust3 (access: 20.10.2014).

Jakubowski M., Sterczyska M., Matysko R., Poreda A. 2014. *Simulation and experimental research on the flow inside a whirlpool separator*. Journal of Food Engineering, 133: 9–15.

Koch D.L., Hill R.J. 2001. *Inertial effects in suspension and porous-media flows*. The Annual Review of Fluid Mechanics, 33: 619–647.

Lee I., Bitog J.P., Se-Woon H., Il-Hwan S., Kyeong-Seok K., Bartzana T., Kacira M. 2013. *The past, present and future of CFD for agro-environmental applications*. Computers and Electronics in Agriculture, 93: 168–183.

Mastersizer 2000 Integrated systems for particle sizing, http://www.malvern.co.uk/ms2000 (access: 8.11.2015).

MODY V., JAKHETE R.M. 1987. *Dust Control Handbook For Minerals Processing*. Department of the Interior. Washington DC, U.S. https://www.osha.gov/dsg/topicss-1ilicacrystalline/dust/dust_control_handbook.html (access: 21.10.2014).

OBERNBERGER I., THEK G. 2010. *The Pellet Handbook the Production and Thermal Utilization of Pellets*. Earthscan, NY, p. 85–108.

XU Z., MICHAELIDES E. 2003. *The effect of particle interactions on the sedimentation process of non-cohesive particles*. International Journal of Multiphase Flow, 29: 959–982.

ZIKANOV O. 2010. *Essential Computational Fluid Dynamics*. Wiley & Sons, New Jersey, p. 86–102.